Effect of homogeneous Fenton combined with electron transfer on the fate of inorganic chlorinated species in synthetic and reclaimed municipal wastewater

Emmanuel Mousset, Lenna Quackenbush, Christine Schondek, Arthur Gerardin-Vergne, Steve Pontvianne, Stephen Kmiotek, Marie-Noëlle Pons

Effect of homogeneous Fenton combined with electron transfer on the fate of inorganic chlorinated species in synthetic and reclaimed municipal wastewater

Emmanuel Mousset[1,*], Lenna Quackenbush[1,2], Christine Schondek[1,2], Arthur Gerardin-Vergne[1], Steve Pontvianne[1], Stephen Kmiotek[2], Marie-Noëlle Pons[1]

[1] Laboratoire Réactions et Génie des Procédés, Université de Lorraine, CNRS, LRGP, F-54000 Nancy, France.

[2] Department of Chemical Engineering, Worcester Polytechnic Institute, Worcester, MA 01609, USA.

Accepted version

ELECTROCHIMICA ACTA

(SI: ISE Topical 2019 Toledo)

*Correspondence to:

Emmanuel MOUSSET: emmanuel.mousset@univ-lorraine.fr ; phone number: +33 (0)3 72 74 37 44

ABSTRACT

This study newly investigates in detail the fate of inorganic chlorinated species and potential interference with other inorganic compounds such as phosphate, inorganic carbon and nitrogenous species during the electro-Fenton treatment of synthetic and reclaimed wastewater. A mathematical model was proposed to validate reaction pathways and rate constants of chlorinated species. The comparison of modeling results with experimental data of both synthetic and real solutions was quite good, with root mean square error (RMSE) values less than 0.084. Upon further testing, the results also showed that adding carbonate, phosphate and inorganic nitrogen species did not affect the chlorate and volatile chlorinated species accumulation subsequent to the decay of chloride ions during electro-Fenton. The established pathway in both synthetic and real chlorinated matrices could help to understand and predict the concentration profiles of chlorinated species in wastewater when implementing such electrocatalysis as a complementary treatment. This work also highlights the need to take into account the management of chlorinated intermediates when implementing this technology at larger scale.

Keywords: electro-oxidation/reduction; electro-Fenton; kinetic modeling; chlorinated inorganic species; reclaimed wastewater

1. Introduction

Water is in high demand due to rising global population, rapid urbanization, increased agriculture, and economic growth while, concurrently, water quality is degrading [1]. As a result of these circumstances, providing people access to clean water becomes more and more challenging every day. Wastewater treatment plants (WWTP) are being increasingly contaminated with micropollutants that are released into the waterbodies [2]. This increase, in combination with industrial discharge and agricultural runoff, result in approximately 80% of wastewater returning to the environment without treatment [1]. Categorized into several groups, micropollutants include pharmaceuticals consumed and discharged by humans, metals from industry, or pesticides used in agriculture [2]. Freshwater in Europe is being contaminated by more than 100,000 registered chemicals. The increasing commonality and production of chemicals coupled with an increase in population and demand for clean drinking water pose new challenges for wastewater treatment facilities [3]. The major biological treatment processes currently being employed at most municipal WWTP are unable to fully degrade many of the organic compounds in the effluent stream [2]. The presence of organic micropollutants in drinking water and surface water is causing great concern for the health of humans and aquatic organisms. Even in low concentrations, organic micropollutants may have negative hormonal, carcinogenic and reproductive impacts in human health and otherwise harm the environment [4].

There are opportunities to decrease this quantity of micropollutants and increase the water quality through actions such as the reuse of treated wastewater by implementing complementary advanced physico-chemical treatment technologies [3]. In this study, the water treatment method of electrolysis is investigated using electro-Fenton conditions, an advanced oxidation process for biorecalcitrant organic pollutants removal in wastewater. The electrochemical advanced oxidation processes (EAOPs) have gain increasing interests for their ability to continuously produce hydroxyl radicals ($^{\bullet}OH$) using low concentration of chemicals or even no reagents by implementing electrocatalysis [5,6]. $^{\bullet}OH$ can react very quickly with biorecalcitrant organic compounds, especially with double C=C bonds, which made them very useful for such water application [7]. EAOPs allow reaching very high degradation and mineralization yields in synthetic or real effluents, as compared to the chemical AOPs [8,9]. Electro-Fenton (EF) has been widely studied due to some advantages compared to chemical Fenton. It allows

regenerating ferric ion (Fe^{3+}) into Fe^{2+} (Eq. 1) and electrogenerating H_2O_2 *in situ* (Eq. 2) through reduction reactions at the cathode.

$$Fe^{3+} + e^- \rightarrow Fe^{2+} \quad (1)$$

$$O_2 + 2H^+ + 2e^- \rightarrow H_2O_2 \quad (2)$$

The combination of Fe^{2+} and H_2O_2 then permits the production of $^{\bullet}OH$ through the Fenton reaction (Eq. 3).

$$Fe^{2+} + H_2O_2 \rightarrow Fe^{3+} + {}^{\bullet}OH + OH^- \quad (3)$$

Numerous investigations have been performed on the degradation/mineralization kinetics study of single pollutant or with cocktail of pollutants in synthetic solution [10–14] while some investigations have been performed in real effluents [15–18]. However, one of the disadvantages of the oxidation processes is the potential to generate harmful by-products, even more harmful than the original pollutants [19,20]. Some efforts have been made to identify and quantify the organic by-products formed during the electrolysis and assess the ecotoxicity. The fate of the inorganic matrix and its influence on kinetics has been barely studied, especially in homogeneous Fenton process combined with direct electro-oxidation/reduction. The concentration profiles of inorganic nitrogen species has been studied in advanced electro-oxidation conditions [21–26] and more recently in electro-Fenton process combined with a modeling study [27]. The evolution of concentration of inorganic chlorinated species has been mainly studied in electro-oxidation process, especially for electro-disinfection purpose [28–36]. Boron-doped diamond (BDD) is well-known to be a non-active anode that has a strong oxidation power, allowing not only the generation of $^{\bullet}OH$, but also the direct oxidation of chloride ions until perchlorate [5].

The concentration profiles of inorganic chlorinated species in homogeneous Fenton combined with electron transfer using an active anode has never been investigated in detail. For the first time, the reaction mechanisms and kinetic pathways of various chlorinated inorganic compounds including volatile species were investigated and supported by a kinetic model study. The influence of phosphate and carbonate has been also investigated and the comparison with reclaimed municipal wastewater effluent was then examined. Through deeper understanding of the potential by-products that can be

created, this study brings new insights on the redox cycle of inorganic chlorinated species in synthetic and real effluent along with emphasizes on the possible unwanted remaining inorganic species after electrolysis.

2. Experimental

2.1. Chemicals

Sodium hypochlorite (NaOCl), chlorite ($NaClO_2$), chlorate ($NaClO_3$) and perchlorate ($NaClO_4$) were supplied by Sigma-Aldrich (Saint-Quentin-Fallavier, France). Sodium carbonate ($NaHCO_3$), sodium hydrogen phosphate (Na_2HPO_4) and sodium chloride (NaCl) were provided by VWR International (Fontenay-sous-Bois, France). Heptahydrated ferrous sulfate ($FeSO_4 \cdot 7H_2O$) and sulfuric acid (H_2SO_4) were purchased from Thermo-Fisher Scientific (Karlsruhe, Germany). All the chemicals were of analytical grade and were used as is.

2.2. Effluent characteristics

The fate of inorganic chlorinated species taking into account Cl^-, $ClOH/ClO^-$, ClO_2^-, ClO_3^-, ClO_4^- and chlorinated volatile species ($Cl_{volatile}$) was determined first in synthetic wastewater to better understand each mechanism independently. A concentration of 150 mg L^{-1} for Cl^- was implemented, which is a representative concentration in reclaimed wastewater [27], while a concentration of 20 mg L^{-1} was used for $ClOH/ClO^-$, ClO_2^-, ClO_3^-, ClO_4^-. The concentration of $Cl_{volatile}$ was estimated by mass balance, considering that Cl^-, $ClOH/ClO^-$, ClO_2^-, ClO_3^- and ClO_4^- were the main stable dissolved inorganic chlorinated species present in the treated solution. The influence of phosphate (PO_4^{3-}) (20 mg L^{-1}) and carbonate (CO_3^{2-}) (20 mg L^{-1}) has been also assessed in synthetic solution, as they can be found in reclaimed wastewater in a range of concentrations that can vary according to the treatment implemented before the exit of the plant. In all experiments, the synthetic solutions were prepared with ultrapure water from a Purelab® water purification system (Veolia Water, Antony, France) with a resistivity higher than 18 MΩ cm at room temperature. The concentration profiles of the inorganic chlorinated species were then monitored in reclaimed wastewater sampled at the outlet of a municipal wastewater treatment plant (Reims, France). The main physico-chemical characteristics of the reclaimed wastewater has been

104 described in a previous study [27]. In order to avoid the presence of any potential residual particulate
105 pollution, the reclaimed wastewater has been filtered (0.45 µm) first before use.
106
107 2.3. Electrolytic treatments
108 Electrolysis experiments were conducted in a 180 mL-undivided cylindrical glass reactor connected to
109 a HAMEG 7042-5 (Beauvais, France) power supply and operated in batch mode at 25 ±1 °C [27]. The
110 current density was set at 2.5 mA cm^{-2}, since it is the average optimal value depicted in previous works
111 in similar electro-Fenton conditions [27,37,38]. Both cathode and anode used for the experiments were
112 made out of carbon felt pieces (Mersen; Gennevilliers, France) having a geometric surface area of 50
113 cm^2. They were pre-conditioned in order to remove any impurity from the surface though a one-hour
114 sonication in a acetone/ultrapure water mixture [39]. Subsequently, they were rinsed with ultrapure
115 water and stored at 60°C for 24 h. The pieces have been renewed for each experiment in order to have a
116 better repeatability and to avoid any contamination by adsorption phenomena that could interfere the
117 subsequent experiment using the same felt. The electrodes were placed in parallel by keeping the inter-
118 electrode distance to 1.5 cm [27]. An active anode, i.e. low O_2 evolution overvoltage (1.6 V vs SHE),
119 has been selected in order to avoid the production of $^{\bullet}OH$ at its surface as previously shown in literature
120 [27,40,41]. It ensured that the only source of $^{\bullet}OH$ could come from the Fenton reaction while only direct
121 electron transfer could occur at cathode and anode [27]. The pH of solution was adjusted to a value of 3
122 with H_2SO_4, which has been found to be optimal for the Fenton process [42], and ferrous iron
123 ($FeSO_4 \cdot 7H_2O$) was maintained at the optimal concentration (0.1 mM) referenced in literature [27,42–
124 44]. A source of O_2 from air for H_2O_2 electrogeneration was supplied continuously throughout the
125 electrolysis. The solutions were continuously stirred at 500 rpm with a magnetic stirrer (Corning PC-
126 410D) for homogeneous mixing. The addition of supporting electrolyte was not required since the
127 average conductivity of synthetic and reclaimed wastewater was around 1 mS cm^{-1} which was high
128 enough. It also minimized the possible interference of the additional electrolyte with the mechanism of
129 oxidation and reduction of the studied species during the electrolytic treatments.
130
131
132

2.4. Analytical procedures

To measure the total organic carbon (TOC), total inorganic carbon (TIC) and total nitrogenous species (TN) a Shimadzu (Marne-La-Vallée, France) V_{CSH} analyzer combined with a TNM-1 analyzer was used. The ion chromatography was conducted on a Dionex/Thermo-Fisher ICS 3000 (Noisy-Le-Grand, France) and measured nitrite (NO_2^-), nitrate (NO_3^-), chloride (Cl^-), chlorite (ClO_2^-), chlorate (ClO_3^-), perchlorate (ClO_4^-), phosphate (PO_4^{3-}) and sulfate (SO_4^{2-}) ions using an AS-19 anion-exchange column in the conditions described previously [27].

Hypochlorous acid and ammonium ions have been quantified by colorimetric method using diethyl-p-phenylene diamine (DPD) (program 80) and salicylate (program 801) procedures, respectively, from Hach kit tests using DR-2400 Hach equipment (Lognes, France).

2.5. Kinetic modeling

MATLAB® modeling software was used to create a kinetic model of the concentration profiles of inorganic chlorinated species. The model used ordinary differential equations (ODE15s) to solve the system. The FMINSEARCH tool of MATLAB® was used to calibrate the model. To assess the fitting of the model in comparison with experimental data, the root mean square error (RMSE), model efficiency (ME) and the index of agreement (IoA) were calculated according to the following equations (Eqs. 4-6) [27,44]:

$$\mathrm{RMSE} = \sqrt{\frac{\sum_{i=1}^{K}(y_i - y_i')^2}{K}} \quad (4)$$

$$\mathrm{ME} = 1 - \frac{\sum_{i=1}^{K}(y_i - y_i')^2}{\sum_{i=1}^{K}(y_i - y_M)^2} \quad (5)$$

$$\mathrm{IoA} = 1 - \frac{\sum_{i=1}^{K}(y_i - y_i')^2}{\sum_{i=1}^{K}(|y_i' - y_M| + |y_i - y_M|)^2} \quad (6)$$

where K is the number of observed values, y_i is the single numerically simulated value, y_i' is the corresponding experimentally observed value, y_M is the average of the numerically simulated values.

3. Results and discussion

Before discussing about the fate of the inorganic chlorinated species, it is important to check whether the sulfate ions added for pH adjustment was involved in the redox reactions or not. A previous study has shown that in the applied conditions the sulfate ions did not have any impact on the reactions [27]. Therefore, it is assumed that only chlorinated species are involved in the results presented in this section.

3.1. Redox cycle of inorganic chlorinated species in synthetic solution

3.1.1. Profiles of single inorganic chlorinated species

Experiments with single inorganic chlorinated species (Cl^-, ClOH, ClO_2^-, ClO_3^-, ClO_4^-) have been performed in synthetic solutions and in acidic media (pH 3). At this pH, hypochlorous acid is the dominant species as compared to hypochlorite ion (ClO^-), since the acid dissociation constant (pKa) of ClOH/ClO^- couple is 7.5 [45]. Therefore, only ClOH was considered in this study. The profiles of Cl^-, ClOH, ClO_2^-, ClO_3^-, ClO_4^- and $Cl_{volatile}$ species as function of the specific charge (Q) are displayed in Fig. 1. $Cl_{volatile}$ could be ascribed to Cl_2, ClO_2 and Cl_2O that were the main volatile inorganic chlorinated species identified in electro-oxidation process with BDD according to a previous study [46]. Moreover, the bubbling applied during the process should facilitate the volatilization of $Cl_{volatile}$.

All the equations, i.e. direct and indirect oxidation/reduction reactions involved in the redox cycle of inorganic chlorinated species, have been represented in Table 1.

Table 1. direct and indirect oxidation/reduction reactions involved in the redox cycle of inorganic chlorinated species.

Reactions			Ref.
(7)		$\mathbf{Cl^-} + 3H_2O \rightarrow \mathbf{ClO_3^-} + 6H^+ + 6e^-$	[47]
(7')		$\mathbf{ClO_3^-} + 6H^+ + 6e^- \rightarrow \mathbf{Cl^-} + 3H_2O$	[47]
(8)	a	$2\mathbf{Cl^-} \rightarrow \mathbf{Cl_2} + 2e^-$	[45]
	b	$\mathbf{Cl^-} + 2H_2O \rightarrow \mathbf{ClO_2} + 4H^+ + 5e^-$	[28]
	c	$2\mathbf{Cl^-} + H_2O \rightarrow \mathbf{Cl_2O} + 2H^+ + 4e^-$	[46]
(8')	a	$\mathbf{Cl_2} + 2e^- \rightarrow 2\mathbf{Cl^-}$	[45]
	b	$\mathbf{ClO_2} + 4H^+ + 5e^- \rightarrow \mathbf{Cl^-} + 2H_2O$	[28]
	c	$\mathbf{Cl_2O} + 2H^+ + 4e^- \rightarrow 2\mathbf{Cl^-} + H_2O$	[46]
(9)		$\mathbf{Cl^-} + {}^\bullet OH \rightarrow \mathbf{ClOH^-}$	[46]
(9')		$\mathbf{ClOH^-} \rightarrow \mathbf{Cl^-} + {}^\bullet OH$	[46]
(10)		$\mathbf{ClO_3^-} + 5Cl^- + 6H^+ \rightarrow 3H_2O + 3\mathbf{Cl_2}$	[48]
(10')		$3\mathbf{Cl_2} + 3H_2O \rightarrow \mathbf{ClO_3^-} + 5Cl^- + 6H^+$	[48]
(11)		$\mathbf{ClO_3^-} + 2H^+ + 2e^- \rightarrow \mathbf{ClO_2^-} + 2H_2O$	[26]
(11')	a	$\mathbf{ClO_2^-} + 2H_2O \rightarrow \mathbf{ClO_3^-} + 2H^+ + 2e^-$	[26]
	b	$\mathbf{ClO_2^-} + {}^\bullet OH \rightarrow {}^\bullet ClO_2 + HO^-$	[26]
	c	${}^\bullet ClO_2 + {}^\bullet OH \rightarrow \mathbf{ClO_3^-} + H^+$	[26]
(12)		$2\mathbf{ClO_3^-} + 4Cl^- + 3/2O_2 + 12H^+ + 6e^- \rightarrow 6\mathbf{ClOH} + 3H_2O$	[26]
(12')	a	$6\mathbf{ClOH} + 3H_2O \rightarrow 2\mathbf{ClO_3^-} + 4Cl^- + 3/2O_2 + 12H^+ + 6e^-$	[26]
	b	$\mathbf{ClOH} + 2\mathbf{ClO_2} + H_2O \rightarrow 2\mathbf{ClO_3^-} + HCl + 2H^+$	[49]
(13)		$\mathbf{ClO_2^-} + 3H^+ + 2e^- \rightarrow \mathbf{ClOH} + H_2O$	[26]
(13')	a	$\mathbf{ClOH} + H_2O \rightarrow \mathbf{ClO_2^-} + 3H^+ + 2e^-$	[26]
	b	$\mathbf{ClOH} + {}^\bullet OH \rightarrow {}^\bullet ClO + H_2O$	[26]
	c	${}^\bullet ClO + {}^\bullet OH \rightarrow \mathbf{ClO_2^-} + H^+$	[26]
(14)		$\mathbf{ClO_2^-} \rightarrow \mathbf{ClO_2} + e^-$	[28]
(14')		$\mathbf{ClO_2} + e^- \rightarrow \mathbf{ClO_2^-}$	[28]

During the electrolysis of chloride ion, only chlorate (Eq. 7) and $Cl_{volatile}$ (Eqs. 8a-8b) accumulated in solution (Fig. 1a).

The oxidation power involved in this process was not high enough to produce perchlorate, which is the inorganic chlorinated compound having the highest oxidation state. This is an interesting feature since this compound is known to be hazardous and has been classified as disinfection by-products [33]. This can be an advantage compared to non-active anode system, such as BDD-based electrolysis, that preferentially produce perchlorate [29,36]. The absence of generation of perchlorate is confirmed through the other experiments performed with ClOH (Fig. 1b), ClO_2^- (Fig. 1c) and ClO_3^- (Fig. 1d). The electrolysis of ClO_4^- itself (Fig. 1d) did not lead to any oxidation or reduction as its concentration remain constant all along the electrolysis, which further emphasized the stability of this compound. Perchlorate

is known to be a stable species that is the inorganic chlorinated end-product in strong oxidation conditions involved in anodic oxidation process [29,50]. During the electrolysis of ClOH, its reduction into chloride (Eq. 9') was rather quick and the decay of ClOH was complete at a specific charge of 0.5 Ah L^{-1}. However, ClOH did not convert quantitatively into Cl^- because the later was oxidized to chlorate at the anode (Eq. 7). ClOH could be also directly oxidized into chlorate (Eq. 12'a) (Fig. 1b).

Contrastingly, chlorite was quickly oxidized into chlorate (Eq. 11'a-11'c) along with the chlorinated volatile production (Eq. 14) (Fig. 1c). $Cl_{volatile}$ seems to be predominantly produced from chlorate according to their respective opposite concentration evolution. This is in agreement with previous results that highlighted the fast formation of $ClO_{2(g)}$ from ClO_2^- (Eq. 14) [28]. The fast decay of chlorite could explain why it was not accumulated in the experiments with Cl^- and ClOH (Eqs. 13'a-13'c) unlike perchlorate that has been found to accumulate in every experiment, except with perchlorate. It is important to note that in acidic condition (pH 3), $HClO_2$ is also present in solution (10%) while ClO_2^- remain predominant (90%), according to their pKa ($HClO_2/ClO_2^-$) of 2.0. It could slightly decrease the ClO_2^- reactivity as compared to experiments performed at neutral pH or in alkaline condition such as anodic oxidation process.

During the electrolysis of chlorate, $Cl_{volatile}$ was the main intermediate, while chloride was produced at lower extent. A reduction reaction (Eq. 7') could occur in acidic media as suggested by previous authors [47].

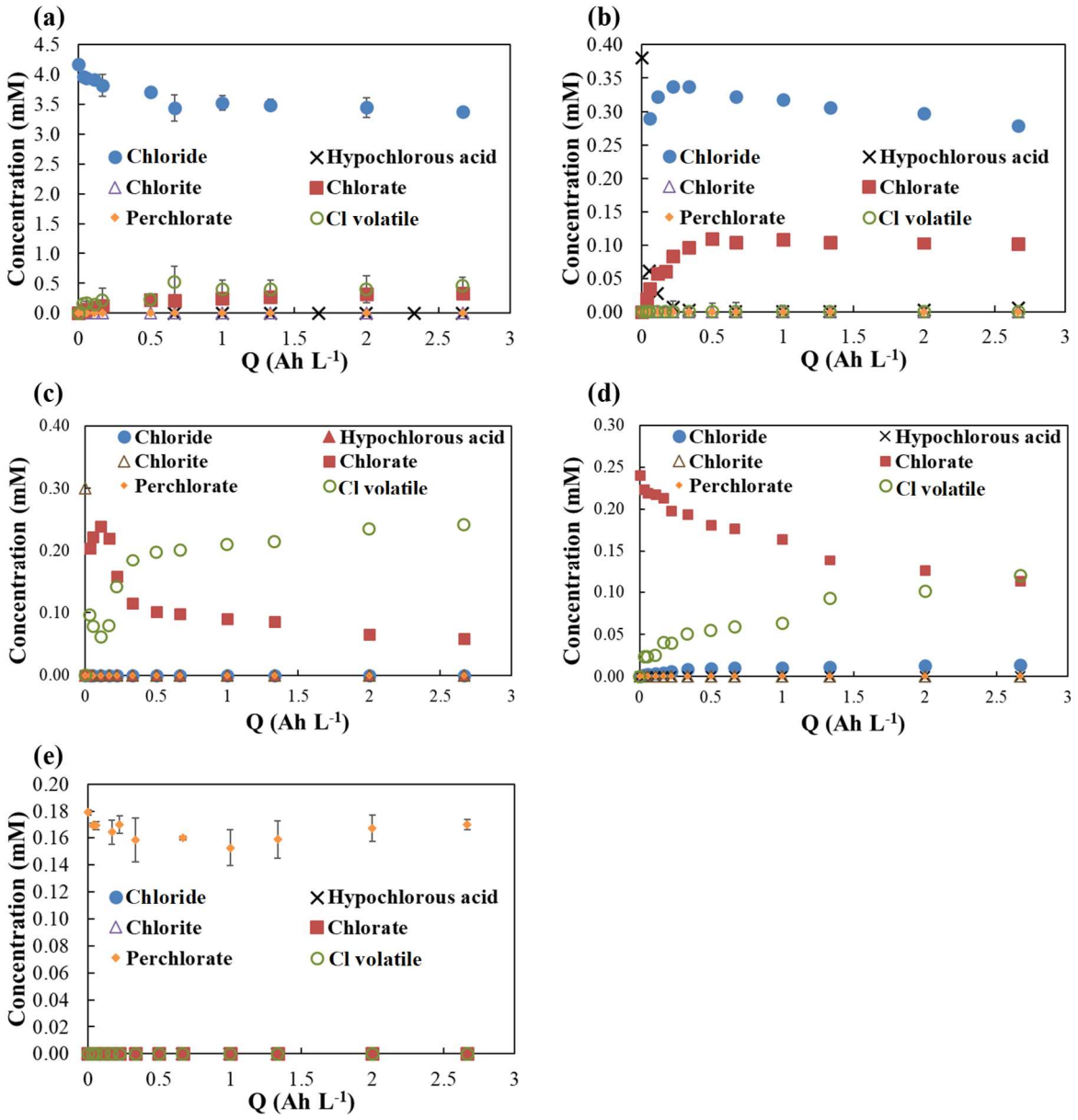

Fig. 1. Profiles of Cl^-, ClOH, ClO_2^-, ClO_3^-, ClO_4^- and $Cl_{volatile}$ in synthetic solutions containing initially (a) Cl^-, (b) ClOH, (c) ClO_2^-, (d) ClO_3^- and (e) ClO_4^- as a function of the applied charge during electro-Fenton treatment. Initial conditions: pH 3, $[Fe^{2+}]$ = 0.1 mM; $[Cl^-]$ = 4.2 mM (a), [ClOH] = 0.37 mM (b), $[ClO_2^-]$ = 0.30 mM (c), $[ClO_3^-]$ = 0.24 mM (d), $[ClO_4^-]$ = 0.18 mM (e).

3.1.2. Profiles and reaction pathway of inorganic chlorinated species mixture

The kinetics evolution of the chlorinated inorganic species has been then determined in an acidic mixture (Fig. 2). The results were in accordance with the profiles depicted in single compound study (section 3.1.1). The chlorate and $Cl_{volatile}$ tended to accumulate while the concentrations of chloride, chlorite and

hypochlorous acid were decreasing and the concentration of perchlorate remained constant. Still, a difference with ClOH profile was noticed, since its decay was not complete after 2.7 Ah L^{-1} (Fig. 2b). With the initial presence of ClO_2^-, the presence of ClO_2 generated from Eq. 14 could also contribute to the oxidation of ClOH (Eq. 12'b). In the meantime, ClOH could be produced from Cl^- oxidation (Eq. 9), ClO_2^- reduction (Eq. 13) and ClO_3^- reduction (Eq. 12), which compensated the rate of ClOH decay.

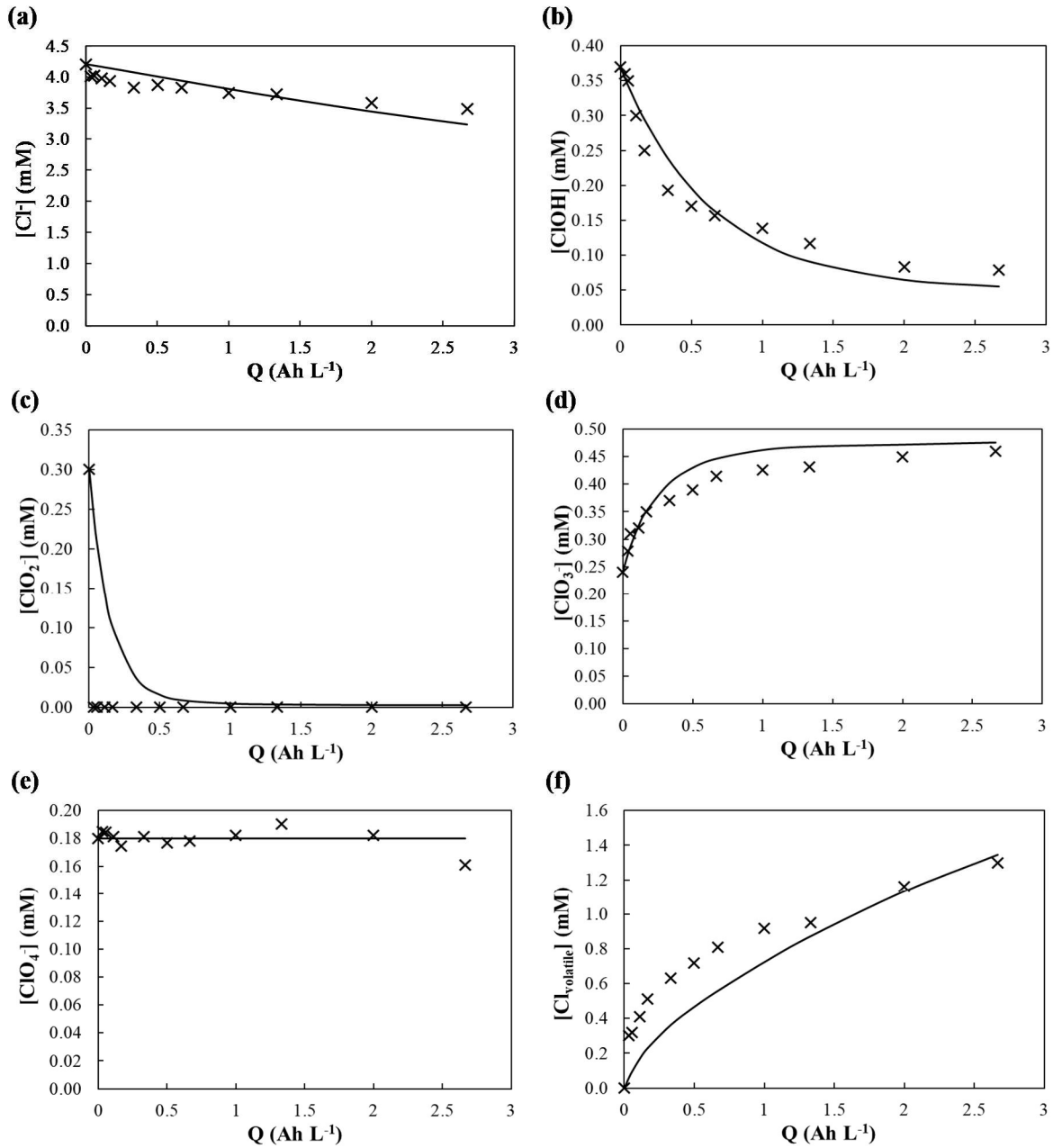

Fig. 2. Comparison of simulated (continuous line) and experimental data (×) about the profiles of (a) Cl^-, (b) ClOH, (c) ClO_2^-, (d) ClO_3^-, (e) ClO_4^- and (f) $Cl_{volatile}$ in synthetic solutions containing initially a mixture of Cl^-, ClOH, ClO_2^-, ClO_3^-, ClO_4^- as a function of the applied specific charge during electro-

Fenton treatment. Initial conditions: pH 3, $[Fe^{2+}]$ = 0.1 mM, $[Cl^-]$ = 4.2 mM, [ClOH] = 0.37 mM, $[ClO_2^-]$ = 0.30 mM, $[ClO_3^-]$ = 0.24 mM, $[ClO_4^-]$ = 0.18 mM.

The experiments made with single chlorinated compounds and with a mixture of them allowed establishing a pathway of the redox cycle of inorganic chlorinated species subjected to electro-oxidation/reduction combined to homogeneous Fenton oxidation with carbon felts electrodes in synthetic acidic solution (Fig. 3).

On the contrary to the pathway given with anodic oxidation using BDD anode [26,51], perchlorate is not appearing in this scheme since the oxidation power was not high enough in the present process. Moreover, the reduction reactions have been considered as well, since electron transfer could occur at both cathode and anode in the electrochemical cell. This reaction pathway highlights the central role of chlorate that directly interact with all the inorganic chlorinated species.

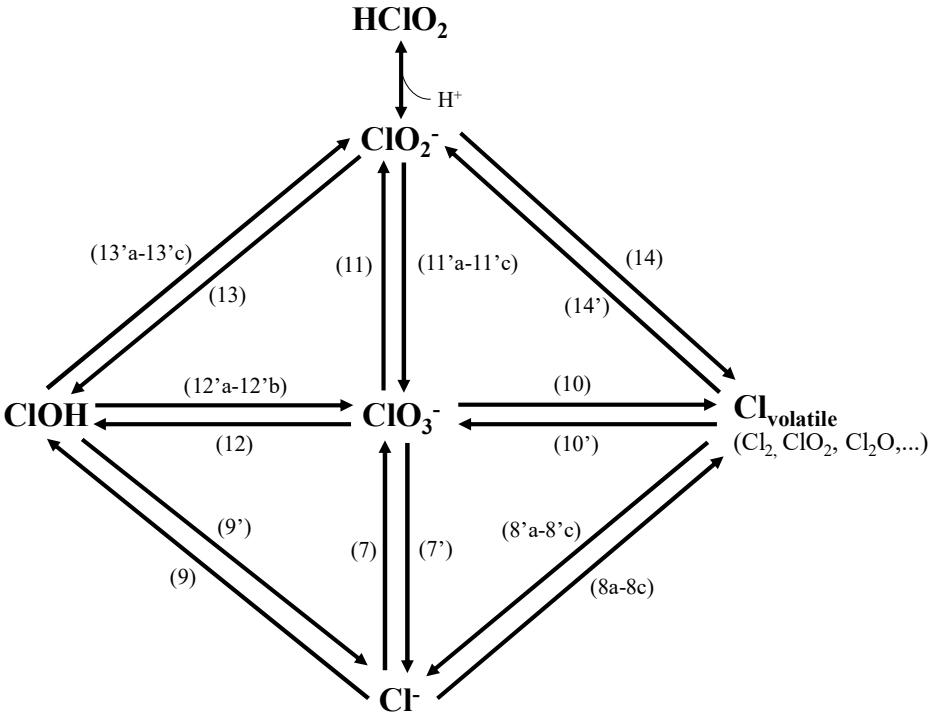

Fig. 3. Scheme of redox cycle of inorganic chlorinated species under electro-oxidation/reduction combined to homogeneous Fenton oxidation with carbon felts electrodes in synthetic acidic solution (pH 3). The equations involved are written in brackets.

3.1.3. Kinetics analysis of inorganic chlorinated species in a synthetic mixture

A kinetic model was proposed based on the results presented in sub-section 3.1.2 that allowed identifying the main chlorinated species involved during the electro-Fenton process.

The order of direct oxidation/reduction reactions was determined according to the initial limiting current density ($j°_{lim}$) (Eq. 15) values compared to the applied current density [52,53].

$$j°_{lim} = nFk_mC_0 \quad (15)$$

where n is the number of electron exchanged, F is the Faraday constant (96485 C mol^{-1}), k_m is the mass transport coefficient (m s^{-1}), C_0 is the initial concentration of the electroactive inorganic chlorinated species (mM).

An average k_m value of 6×10^{-6} m s^{-1} has been taken into account, since it is the common value of the mass transport of species towards electrodes in such electrochemical reactor [39,54]. All the $j°_{lim}$ values were below 1.5 mA cm^{-2}, considering the oxidation of Cl^- into ClO_3^- (Eq. 7). This reaction involves the highest number of electrons exchanged and the highest initial concentration of compounds ($[Cl^-]$ = 2.4 mM), indicating that all other direct oxidation/reduction reactions led to lower $j°_{lim}$. Thus, the applied current density (2.5 mA cm^{-2}) was always higher than $j°_{lim}$. Consequently, the mass transport was the rate-limiting step compared to charge transfer mechanism [52,53]. The rate (r) of direct oxidation/reduction reactions under mass transport control can be expressed as follow (Eq. 16) [52,53]:

$$r = Ak_mC \quad (16)$$

where A is the surface area of the electrode, C is the concentration during the electrolysis of the species that react by direct oxidation/reduction reaction.

Considering Eq. 16, the kinetic of reaction is a first order towards C, the other parameters being constants. It corroborated the kinetic analysis suggested in previous studies that involved first order kinetics for direct oxidation/reduction reactions [24,27]. In addition, based on the quasi-steady state approximation towards $^{\bullet}OH$ concentration, a pseudo-first order kinetic model has been also considered for the reactions between inorganic chlorinated species and $^{\bullet}OH$ [27,42].

Therefore, the following system of differential equations considering first order kinetics was proposed to model the reaction kinetics of the species during electrolysis (Eqs. 17-22):

$$\frac{d[Cl^-]}{dt} = k'_1[ClO_3^-] + k'_2[Cl_{gas}] + k'_3[ClOH] - (k_1 + k_2 + k_3)[Cl^-] \quad (17)$$

$$\frac{d[ClOH]}{dt} = k_3[Cl^-] + k_7[ClO_2^-] + k_6[ClO_3^-] - (k'_3 + k'_6 + k'_7)[ClOH] \quad (18)$$

$$\frac{d[ClO_2^-]}{dt} = k'_7[ClOH] + k'_8[Cl_{gas}] + k_5[ClO_3^-] - (k'_5 + k_7 + k_8)[ClO_2^-] \quad (19)$$

$$\frac{d[ClO_3^-]}{dt} = k_1[Cl^-] + k'_4[Cl_{gas}] + k'_6[ClOH] + k'_5[ClO_2^-] - (k'_1 + k_4 + k_5 + k_6)[ClO_3^-] \quad (20)$$

$$\frac{d[ClO_4^-]}{dt} = 0 \quad (21)$$

$$\frac{d[Cl_{gas}]}{dt} = k_2[Cl^-] + k_4[ClO_3^-] + k_8[ClO_2^-] - (k'_2 + k'_4 + k'_8)[Cl_{gas}] \quad (22)$$

The main reactions implemented in the system are presented in Table 1. The mathematical model has been compared with the experimental data for chloride, hypochlorous acid, chlorite, chlorate, perchlorate and volatile chlorinated species and the results are displayed in Fig. 2. After calibration of the model, the rate constant values (expressed in s^{-1}) could be estimated (Table 2).

Table 2. Estimated kinetic constants values from the model.

Constant	Chlorinated species involved and direction of reaction	Equations involved	Rate constant value (s^{-1})
k_1	$Cl^- \rightarrow ClO_3^-$	(7)	1.54×10^{-5}
k'_1	$ClO_3^- \rightarrow Cl^-$	(7')	3.86×10^{-7}
k_2	$Cl^- \rightarrow Cl_{volatile}$	(8a-8b)	1.06×10^{-5}
k'_2	$Cl_{volatile} \rightarrow Cl^-$	(8'a-8'b)	1.74×10^{-5}
k_3	$Cl^- \rightarrow ClOH$	(9)	1.93×10^{-7}
k'_3	$ClOH \rightarrow Cl^-$	(9')	9.64×10^{-5}
k_4	$ClO_3^- \rightarrow Cl_{volatile}$	(10)	1.74×10^{-4}
k'_4	$Cl_{volatile} \rightarrow ClO_3^-$	(10')	2.89×10^{-5}
k_5	$ClO_3^- \rightarrow ClO_2^-$	(11)	9.64×10^{-7}
k'_5	$ClO_2^- \rightarrow ClO_3^-$	(11'a-11'c)	3.86×10^{-4}
k_6	$ClO_3^- \rightarrow ClOH$	(12)	2.89×10^{-5}
k'_6	$ClOH \rightarrow ClO_3^-$	(12'a-12'b)	1.54×10^{-4}
k_7	$ClO_2^- \rightarrow ClOH$	(13)	3.86×10^{-7}
k'_7	$ClOH \rightarrow ClO_2^-$	(13'a-13'c)	3.86×10^{-5}
k_8	$ClO_2^- \rightarrow Cl_{volatile}$	(14)	9.64×10^{-4}
k'_8	$Cl_{volatile} \rightarrow ClO_2^-$	(14')	9.64×10^{-7}

The validity of the model was tested to see how well the theoretical curve fit the experimental data by calculating the RMSE, ME and IoA. A model that perfectly fits the data would have a RMSE value of zero and ME and IoA values of one. The RMSE, ME and IoA values for the model are shown in Table

296 3. RMSE, ME and IoA were below 0.084 and higher than 0.919 and 0.991, respectively, descripting a
297 good correlation considering the sixteen rate constants that have been taken into account.
298 The estimated values of parameters were ranging from 1.93×10^{-7} s^{-1} to 9.64×10^{-4} s^{-1}. The highest rate
299 was attributed to the conversion of ClO_2^- into $Cl_{volatile}$ (i.e. $ClO_{2(g)}$), which corroborates the fast
300 conversion observed with single species in section 3.1.1. The oxidation of ClO_2^- into ClO_3^- was also
301 very quick according to the rate constant (3.86×10^{-4} s^{-1}), which confirmed the fast decay of ClO_2^-
302 compared to the other species during the electrolysis.
303
304 **Table 3.** Efficiency of the kinetic model in comparison with experimental data obtained in synthetic
305 solution.

	RMSE	**ME**	**IoA**
Cl^- curve	0.042	0.959	0.990
ClOH curve	0.053	0.940	0.990
ClO_2^- curve	0.084	0.919	0.941
ClO_3^- curve	0.025	0.970	0.994
ClO_4^- curve	0.021	0.992	0.999
$Cl_{volatile}$ curve	0.070	0.976	0.989

306
307 The model proposed in this study allowed confirming the pathway proposed in Fig. 3. This scheme and
308 the model is valid in synthetic solution with inorganic chlorinated species only, considering no
309 interference with other species that could be present in the effluent. The possible matrix effect has been
310 studied in the following sections to evaluate these aspects.
311
312 3.2. Influence of additional inorganic species on concentration profile of chlorinated species
313 The possible impact of phosphate ion and inorganic carbon has not been studied previously, though
314 these species are commonly present in municipal wastewater effluents along with chloride ions [27,39].
315 The influence of phosphate on the oxidation of chloride was determined by comparing the results from
316 an experiment with initial additions of chloride and phosphate to an experiment with only chloride added
317 initially (Figs. 4a and 4b). When comparing the normalized chloride concentrations of the experiment
318 with phosphate to the experiment without phosphate, the values fell within the standard deviation of
319 each other (Fig. 4a). Both experiments followed a similar trend with a decreasing amount of chloride as
320 applied specific charge increased until 20% of Cl^- removal after 2.7 Ah L^{-1}. The kinetics of the evolution

of inorganic chlorinated species for both experiments are illustrated in Fig. 4b. ClO_3^- was the only species quantified in the samples in both experiments, which is in agreement with single chloride experiments (Fig. 1a). Both experiments followed the same trend and the same kinetics considering the standard deviation, i.e. absence of chlorate initially and increasing over applied specific charge until a plateau around 0.24 mM. Therefore, phosphate did not have any impact on the redox evolution of inorganic chlorinated species in such electro-Fenton conditions. It seems that perphosphate ($P_2O_8^{4-}$) was not produced during the electrolysis unlike in advanced electro-oxidation process (Eqs. 23-24) as the phosphate concentration remained constant all along the treatment and $P_2O_8^{4-}$ could have oxidized chlorinated species.

$$PO_4^{3-} \rightarrow PO_4^{2-\bullet} + e^- \quad (23)$$

$$2\ PO_4^{2-\bullet} \rightarrow P_2O_8^{4-} \quad (24)$$

The operating conditions may not be strong enough to allow PO_4^{3-} oxidation. It is also important to note that the predominant species at pH 3 are phosphoric acid (H_3PO_4) and $H_2PO_4^-$ whose pKa is 2.15. In this context, the oxidation of H_3PO_4 or $H_2PO_4^-$ species could be more difficult.

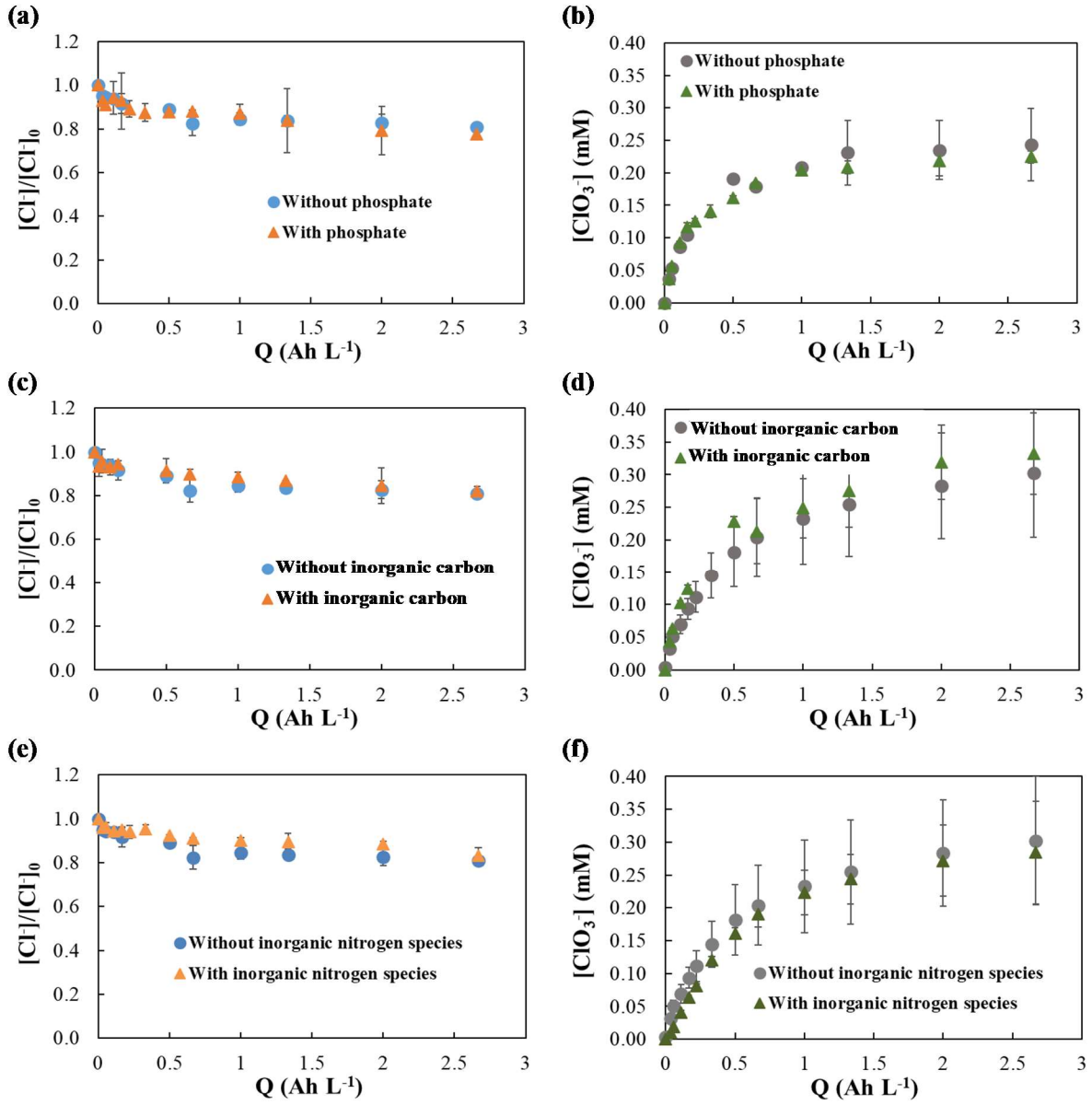

Fig. 4. Effect of phosphate ((a) and (b)), inorganic carbon ((c) and (d)) and inorganic nitrogen species ((e) and (f)) contents on the decay of Cl^- normalized to the initial Cl^- concentration ($[Cl^-]_0$) ((a), (c) and (e)) and on the generation of ClO_3^- ((b), (d) and (f)) in synthetic solutions as a function of the applied specific charge during electro-Fenton treatment. Initial conditions: pH 3, $[Fe^{2+}]$ = 0.1 mM, $[Cl^-]$ = 4.2 mM; $[PO_4^{3-}]$ = 0.21 mM ((a) and (b)), $[CO_3^{2-}]$ = 0.33 mM ((c) and (d)), $[NH_4^+]$ = 0.8 mM ((e) and (f)), $[NO_3^-]$ = 0.37 mM ((e) and (f)), $[NO_2^-]$ = 0.19 mM ((e) and (f)).

Similarly, the effect of inorganic carbon on the concentration profiles of inorganic chlorinated species was also negligible (Figs. 4c and 4d). In acidic condition the predominant inorganic carbon species present in solution is carbonic acid (H_2CO_3), according to the pKa of H_2CO_3/HCO_3^- couple that equal

348 6.3. Both acidic and milder oxidative stress conditions compared to the anodic oxidation technology
349 might limit the formation of percarbonate (Eqs. 25-26) that could have played a role in the oxidation of
350 chlorinated species otherwise.

351 $CO_3^{2-} \rightarrow CO_3^{-\bullet} + e^-$ (25)

352 $2\ CO_3^{-\bullet} \rightarrow C_2O_6^{2-}$ (26)

353

354 It further highlights that in this acidic condition, the formation of calcium carbonate ($CaCO_3$) at the
355 cathode due to local pH increase [26] can be avoided. In the presence of Ca^{2+} and CO_3^{2-}, which is the
356 case of reclaimed wastewater [27,39], this local precipitation is frequent and cause scaling effect that
357 can impede the electrolysis.
358 The influence of inorganic nitrogen species has been also tested using concentration of 0.8 mM, 0.37
359 mM and 0.19 mM for NH_4^+, NO_3^- and NO_2^- respectively, which corresponds to the concentration
360 employed in a previous study [27]. The results are shown in Figs. 4e and 4f and the same trends and
361 kinetics of chloride and chlorate concentrations where observed regardless of the presence or absence
362 of nitrogen species. However, the kinetics evolution of nitrogen species is impacted by the presence of
363 chlorinated species as previously shown in electro-Fenton condition [27]. The ammonia tends to
364 decrease due to the formation of monochloramine (NH_2Cl), dichloramine ($NHCl_2$) and trichloramine
365 (NCl_3) with ClOH, while nitrate tends to accumulate in solution [27].

366

367 Thus, the presence in the initial effluent of phosphate, inorganic carbon and inorganic nitrogen species
368 should not affect the concentration profiles and the proposed pathway of the inorganic chlorinated
369 species in electro-Fenton condition. This is verified in reclaimed wastewater in the following section
370 3.3.

371

372 3.3. Validation of the suggested model on the concentration profiles of inorganic chlorinated
373 species in reclaimed wastewater

374 Experiments have been performed with reclaimed wastewater from the outlet of a municipal wastewater
375 treatment plant in Reims, France. The characteristics of the initial effluent are given in a previous paper
376 [27]. The inorganic chlorinated species have been monitored and only chloride and chlorate were

377 detected in the samples from the wastewater electrolysis and their concentrations are graphed in Fig. 5a
378 and Fig. 5b, while $Cl_{volatile}$ is plotted in Fig. 5c. The model that has been proposed in section 3.1.2 has
379 been applied for the experiments with real effluent and the results are depicted in Figs. 5a-c. The same
380 kinetic rate constant values and ordinary differential equations were used. The model fitted quite well
381 the experimental concentrations of the chlorinated species. RMSE, ME and IoA were lower than 0.071
382 and higher than 0.910 and 0.937, respectively (Table 4). It further confirmed that phosphate, inorganic
383 carbon contents and nitrogenous species were not impacting the fate of chloride and chlorate species.
384 The pathway proposed in Fig. 3 could be then validated with real wastewater.
385

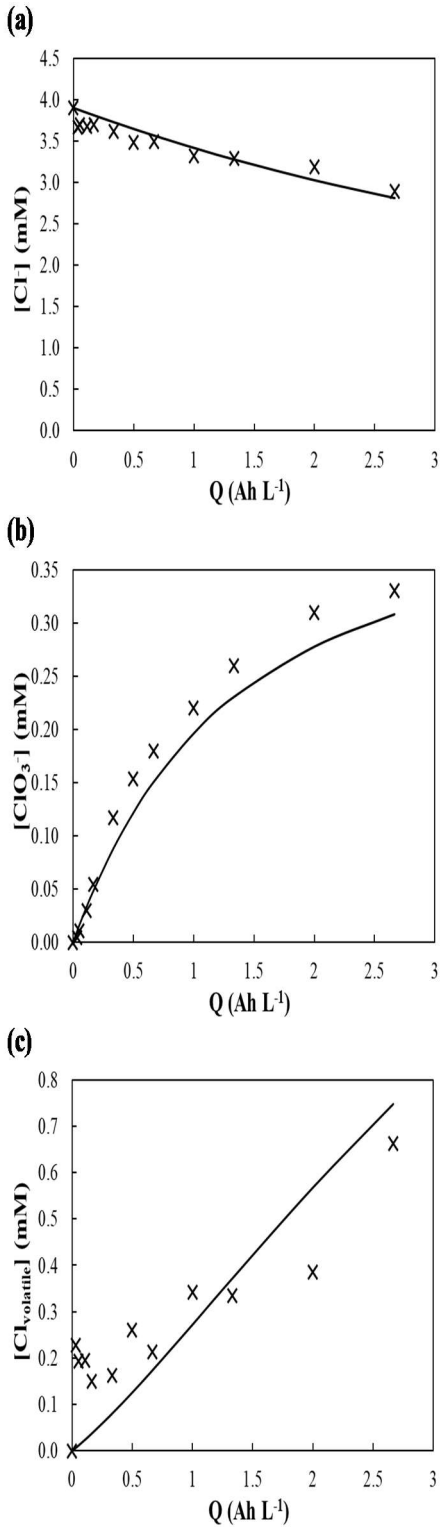

386

387 **Fig. 5.** Comparison of simulated (continuous line) and experimental data (×) about the profiles of (a)

388 Cl^-, (b) ClO_3^- and (c) $Cl_{volatile}$ in reclaimed wastewater as a function of the applied specific charge

389 during electro-Fenton treatment. Initial conditions: pH 3, $[Fe^{2+}]$ = 0.1 mM.

390

391

392 **Table 4.** Validation of the kinetic model applied for reclaimed wastewater.

	RMSE	ME	IoA
Cl^- curve	0.059	0.990	0.991
ClO_3^- curve	0.034	0.990	0.997
$Cl_{volatile}$ curve	0.071	0.910	0.937

393

394

395 ## 4. Conclusions

396 For the first time, the concentration profiles of inorganic chlorinated species in synthetic and reclaimed
397 municipal wastewater in electro-Fenton process have been investigated in detail. The redox cycles of
398 chloride, hypochlorous acid, chlorite, chlorate, perchlorate and volatile chlorinated species have been
399 established. A kinetic model considering first order kinetics and sixteen rate constants has been
400 proposed. After calibration and validation of the model with experimental data obtained in synthetic
401 solution, the model has been further validated with a real solution. A reaction pathway has been
402 suggested for both synthetic and reclaimed wastewater.

403 The acidic and mild oxidation conditions compared to anodic oxidation with non-active anode permit
404 to avoid the interference of phosphate, carbonate and inorganic nitrogen species with the redox cycles
405 of inorganic chlorinated species. Furthermore, perchlorate could not accumulate unlike in advanced
406 electro-oxidation. However, chlorate and volatile chlorinated species were still accumulating with the
407 applied specific charge for all tested solutions. In this context, these intermediates need to be carefully
408 assessed during the electro-Fenton treatment of real chlorinated effluents.

409

410

411 ## References

412 [1] UNESCO, Wastewater, The Untapped Resource. United Nations World Water Development
413 Report, 2017.

414 [2] S.D. Richardson, S.Y. Kimura, Water Analysis: Emerging Contaminants and Current Issues,
415 Anal. Chem. 88 (2016) 546–582.

416 [3] R.I.L. Eggen, J. Hollender, A. Joss, M. Schärer, C. Stamm, Reducing the discharge of
417 micropollutants in the aquatic environment: The benefits of upgrading wastewater treatment
418 plants, Environ. Sci. Technol. 48 (2014) 7683–7689.

[4] L. Kovalova, H. Siegrist, U. von Gunten, J. Eugster, M. Hagenbuch, A. Wittmer, R. Moser, C.S. McArdell, Elimination of micropollutants during post-treatment of hospital wastewater with powdered activated carbon, ozone, and UV., Environ. Sci. Technol. 47 (2013) 7899–7908.

[5] F.C. Moreira, R.A.R. Boaventura, E. Brillas, V.J.P. Vilar, Electrochemical advanced oxidation processes: A review on their application to synthetic and real wastewaters, Appl. Catal. B Environ. 202 (2017) 217–261.

[6] C.A. Martínez-Huitle, M.A. Rodrigo, I. Sirés, O. Scialdone, Single and coupled electrochemical processes and reactors for the abatement of organic water pollutants : A critical review, Chem. Rev. 115 (2015) 13362–13407.

[7] E. Mousset, N. Oturan, M.A. Oturan, An unprecedented route of OH radical reactivity evidenced by an electrocatalytical process: Ipso-substitution with perhalogenocarbon compounds, Appl. Catal. B Environ. 226 (2018) 135–146.

[8] N. Oturan, E. Brillas, M.A. Oturan, Unprecedented total mineralization of atrazine and cyanuric acid by anodic oxidation and electro-Fenton with a boron-doped diamond anode, Environ. Chem. Lett. 10 (2012) 165–170.

[9] P. Cañizares, R. Paz, C. Sáez, M.A. Rodrigo, Costs of the electrochemical oxidation of wastewaters: a comparison with ozonation and Fenton oxidation processes., J. Environ. Manage. 90 (2009) 410–420.

[10] E. Mousset, N. Oturan, E.D. van Hullebusch, G. Guibaud, G. Esposito, M.A. Oturan, Influence of solubilizing agents (cyclodextrin or surfactant) on phenanthrene degradation by electro-Fenton process - Study of soil washing recycling possibilities and environmental impact, Water Res. 48 (2014) 306–316.

[11] H. Monteil, Y. Péchaud, N. Oturan, M.A. Oturan, A review on efficiency and cost effectiveness of electro- and bio-electro-Fenton processes: Application to the treatment of pharmaceutical pollutants in water, Chem. Eng. J. (2018) 1–30.

[12] L. Feng, N. Oturan, E.D. van Hullebusch, G. Esposito, M.A. Oturan, Degradation of anti-inflammatory drug ketoprofen by electro-oxidation: comparison of electro-Fenton and anodic oxidation processes., Environ. Sci. Pollut. Res. Int. 21 (2014) 8406–8416.

[13] S. Garcia-Segura, R. Salazar, E. Brillas, Mineralization of phthalic acid by solar photoelectro-

Fenton with a stirred boron-doped diamond/air-diffusion tank reactor: Influence of Fe^{3+} and Cu^{2+} catalysts and identification of oxidation products, Electrochim. Acta. 113 (2013) 609–619.

[14] I.F. Mena, S. Cotillas, E. Díaz, C. Sáez, Á.F. Mohedano, M.A. Rodrigo, Influence of the supporting electrolyte on the removal of ionic liquids by electrolysis with diamond anodes, Catal. Today. 313 (2018) 203–210.

[15] E. Mousset, D. Huguenot, E.D. Van Hullebusch, N. Oturan, G. Guibaud, G. Esposito, M.A. Oturan, Impact of electrochemical treatment of soil washing solution on PAH degradation efficiency and soil respirometry, Environ. Pollut. 211 (2016) 354–362.

[16] N. Oturan, E.D. Van Hullebusch, H. Zhang, L. Mazeas, H. Budzinski, K. Le Menach, M.A. Oturan, Occurrence and removal of organic micropollutants in landfill leachates treated by electrochemical advanced oxidation processes, Environ. Sci. Technol. 49 (2015) 12187–12196.

[17] S. Garcia-Segura, J.D. Ocon, M.N. Chong, Electrochemical oxidation remediation of real wastewater effluents — A review, Process Saf. Environ. Prot. 113 (2018) 48–67.

[18] E. Mousset, Z. Wang, H. Olvera-Vargas, O. Lefebvre, Advanced electrocatalytic pre-treatment to improve the biodegradability of real wastewater from the electronics industry — A detailed investigation study, J. Hazard. Mater. 360 (2018) 552–559.

[19] E. Mousset, N. Oturan, E.D. van Hullebusch, G. Guibaud, G. Esposito, M.A. Oturan, Treatment of synthetic soil washing solutions containing phenanthrene and cyclodextrin by electro-oxidation. Influence of anode materials on toxicity removal and biodegradability enhancement, Appl. Catal. B Environ. 160–161 (2014) 666–675.

[20] N. Barhoumi, N. Oturan, H. Olvera-Vargas, E. Brillas, A. Gadri, S. Ammar, M.A. Oturan, Pyrite as a sustainable catalyst in electro-Fenton process for improving oxidation of sulfamethazine. Kinetics, mechanism and toxicity assessment, Water Res. 94 (2016) 52–61.

[21] A. Kapalka, L. Joss, Á. Anglada, C. Comninellis, K.M. Udert, Direct and mediated electrochemical oxidation of ammonia on boron-doped diamond electrode, 12 (2010) 1714–1717.

[22] A. Kapałka, S. Fierro, Z. Frontistis, A. Katsaounis, S. Neodo, O. Frey, N. de Rooij, K.M. Udert, C. Comninellis, Electrochemical oxidation of ammonia (NH_4^+/NH_3) on thermally and electrochemically prepared IrO_2 electrodes, Electrochim. Acta. 56 (2011) 1361–1365.

[23] E. Lacasa, J. Llanos, P. Cañizares, M.A. Rodrigo, Electrochemical denitrificacion with chlorides using DSA and BDD anodes, Chem. Eng. J. 184 (2012) 66–71.

[24] G. Pérez, R. Ibáñez, A.M. Urtiaga, I. Ortiz, Kinetic study of the simultaneous electrochemical removal of aqueous nitrogen compounds using BDD electrodes, Chem. Eng. J. 197 (2012) 475–482.

[25] M.J.M. De Vidales, M. Millán, C. Sáez, P. Cañizares, M.A. Rodrigo, What happens to inorganic nitrogen species during conductive diamond electrochemical oxidation of real wastewater ?, Electrochem. Commun. 67 (2016) 65–68.

[26] Y. Lan, C. Coetsier, C. Causserand, K. Groenen Serrano, On the role of salts for the treatment of wastewaters containing pharmaceuticals by electrochemical oxidation using a boron doped diamond anode, Electrochim. Acta. 231 (2017) 309–318.

[27] E. Mousset, S. Pontvianne, M.-N. Pons, Fate of inorganic nitrogen species under homogeneous Fenton combined with electro-oxidation/reduction treatments in synthetic solutions and reclaimed municipal wastewater, Chemosphere. 201 (2018) 6–12.

[28] H. Bergmann, A.S. Koparal, The formation of chlorine dioxide in the electrochemical treatment of drinking water for disinfection, Electrochim. Acta. 50 (2005) 5218–5228.

[29] M.E.H. Bergmann, J. Rollin, T. Iourtchouk, The occurrence of perchlorate during drinking water electrolysis using BDD anodes, Electrochim. Acta. 54 (2009) 2102–2107.

[30] H. Bergmann, A.T. Koparal, A.S. Koparal, F. Ehrig, The influence of products and by-products obtained by drinking water electrolysis on microorganisms, Microchem. J. 89 (2008) 98–107.

[31] M.E.H. Bergmann, J. Rollin, Product and by-product formation in laboratory studies on disinfection electrolysis of water using boron-doped diamond anodes, Catal. Today. 124 (2007) 198–203.

[32] M.E.H. Bergmann, A.S. Koparal, T. Iourtchouk, Electrochemical Advanced oxidation processes, formation of halogenate and perhalogenate species: A critical review, Crit. Rev. Environ. Sci. Technol. 44 (2014) 348–390.

[33] C.D.N. Brito, D.M. de Araújo, C.A. Martínez-Huitle, M.A. Rodrigo, Understanding active chlorine species production using boron doped diamond films with lower and higher sp^3/sp^2 ratio, Electrochem. Commun. 55 (2015) 34–38.

[34] J. Llanos, S. Cotillas, P. Cañizares, M.A. Rodrigo, Conductive diamond sono-electrochemical disinfection (CDSED) for municipal wastewater reclamation., Ultrason. Sonochem. 22 (2015) 493–498.

[35] A. Cano, P. Cañizares, C. Barrera, C. Sáez, M.A. Rodrigo, Use of low current densities in electrolyses with conductive-diamond electrochemical — Oxidation to disinfect treated wastewaters for reuse, Electrochem. Commun. 13 (2011) 1268–1270.

[36] A. Cano, P. Cañizares, C. Barrera-Díaz, C. Sáez, M.A. Rodrigo, Use of conductive-diamond electrochemical-oxidation for the disinfection of several actual treated wastewaters, Chem. Eng. J. 211–212 (2012) 463–469.

[37] M. Panizza, M.A. Oturan, Degradation of Alizarin Red by electro-Fenton process using a graphite-felt cathode, Electrochim. Acta. 56 (2011) 7084–7087.

[38] A. Dirany, I. Sirés, N. Oturan, A. Ozcan, M.A. Oturan, Electrochemical treatment of the antibiotic sulfachloropyridazine: kinetics, reaction pathways, and toxicity evolution, Environ. Sci. Technol. 46 (2012) 4074–4082.

[39] E. Mousset, M. Puce, M.-N. Pons, Advanced electro-oxidation with boron-doped diamond for acetaminophen removal from real wastewater in a microfluidic reactor – Kinetics and mass transfer studies, ChemElectroChem. 6 (2019) 2908–2916.

[40] E. Mousset, Z. Wang, O. Lefebvre, Electro-Fenton for control and removal of micropollutants – process optimization and energy efficiency, Water Sci. Technol. 74 (2016) 2068–2074.

[41] M. Panizza, G. Cerisola, Direct and mediated anodic oxidation of organic pollutants, Chem. Rev. 109 (2009) 6541–6569.

[42] E. Brillas, I. Sirés, M.A. Oturan, Electro-Fenton process and related electrochemical technologies based on Fenton's reaction chemistry, Chem. Rev. 109 (2009) 6570–6631.

[43] I. Sirés, E. Brillas, M.A. Oturan, M.A. Rodrigo, M. Panizza, Electrochemical advanced oxidation processes: today and tomorrow. A review., Environ. Sci. Pollut. Res. 21 (2014) 8336–8367.

[44] E. Mousset, L. Frunzo, G. Esposito, E.D. van Hullebusch, N. Oturan, M.A. Oturan, A complete phenol oxidation pathway obtained during electro-Fenton treatment and validated by a kinetic model study, Appl. Catal. B Environ. 180 (2016) 189–198.

[45] Y.J. Jung, K.W. Baek, B.S. Oh, J.W. Kang, An investigation of the formation of chlorate and

perchlorate during electrolysis using Pt/Ti electrodes: The effects of pH and reactive oxygen species and the results of kinetic studies, Water Res. 44 (2010) 5345–5355.

[46] E. Mostafa, P. Reinsberg, S. Garcia-Segura, H. Baltruschat, Chlorine species evolution during electrochlorination on boron-doped diamond anodes: In-situ electrogeneration of Cl_2, Cl_2O and ClO_2, Electrochim. Acta. 281 (2018) 831–840.

[47] G.M. Brown, The reduction of chlorate and perchlorate ions at an active titanium electrode, J. Electroanal. Chem. 198 (1986) 319–330.

[48] M. Tian, L. Yang, J. Wang, Z. Li, S. Chen, Degradation of p-nitrophenol affected by synergy of indirect and direct electrooxidation, Adv. Mater. Res. 518–523 (2012) 295–298.

[49] B. Michele, P.S. Fair, D.P. Hautman, Occurrence of chlorate in hypochlorite solutions used for drinking water disinfection, Environ. Sci. Technol. 26 (1992) 1663–1665.

[50] A. Sánchez-Carretero, C. Sáez, P. Cañizares, M.A. Rodrigo, Electrochemical production of perchlorates using conductive diamond electrolyses, Chem. Eng. J. 166 (2011) 710–714.

[51] B.P. Chaplin, Critical review of electrochemical advanced oxidation processes for water treatment applications., Environ. Sci. Process. Impacts. 16 (2014) 1182–1203.

[52] M. Panizza, P.A. Michaud, G. Cerisola, C. Comninellis, Anodic oxidation of 2-naphthol at boron-doped diamond electrodes, J. Electroanal. Chem. 507 (2001) 206–214.

[53] E. Mousset, Y. Pechaud, N. Oturan, M.A. Oturan, Charge transfer/mass transport competition in advanced hybrid electrocatalytic wastewater treatment: Development of a new current efficiency relation, Appl. Catal. B Environ. 240 (2019) 102–111.

[54] E.V. dos Santos, S.F.M. Sena, D.R. da Silva, S. Ferro, A. De Battisti, C.A. Martínez-Huitle, Scale-up of electrochemical oxidation system for treatment of produced water generated by Brazilian petrochemical industry, Environ. Sci. Pollut. Res. 21 (2014) 8466–8475.